Differential Recognition and Activation Thresholds in Human Autoreactive GAD-Specific T-Cells

Roberto Mallone,[1] Sharon A. Kochik,[1] Elsa M. Laughlin,[1] Vivian H. Gersuk,[1] Helena Reijonen,[1] William W. Kwok,[1] and Gerald T. Nepom[1,2]

The activation requirements of autoreactive CD4$^+$ T-cells were investigated in GAD65-specific HLA-DR0401–restricted clones derived from a diabetic patient using major histocompatibility complex (MHC) class II tetramers (TMrs) as stimulating agents. Despite the fact that TMrs loaded with an immunodominant-altered GAD peptide (TMr-GAD) bound a limited number of T-cell receptors, they were capable of efficiently delivering activation signals. These signals ranged from the early steps of phospholipase C (PLC)-γ_1 phosphorylation and Ca^{2+} mobilization to more complex events, such as CD69 upregulation, cytokine mRNA transcription and secretion, and proliferation. All the effects triggered by TMr-GAD were dose dependent. On the contrary, [^{3}H]-thymidine incorporation decreased at high TMr-GAD concentrations because of activation-induced cell death (AICD) after initial proliferation. Lower-avidity clones (as defined by TMr-GAD binding) were less sensitive to activation as well as less susceptible to AICD compared with higher-avidity clones. Induction of apoptosis is a potential immunomodulatory target for therapeutic applications of MHC class II multimers, but the relative resistance of low-avidity T-cells may limit its benefits. *Diabetes* 53:971–977, 2004

The Ag-specific T-cell receptor (TCR) is capable of transducing signals after ligand interactions with a wide range of specificity and affinity. The intrinsic TCR propensity for cross-reactivity establishes a threshold for antigen recognition, permitting a variety of different peptides, including some autoantigens, to satisfy the structural requirements for an activation signal (1). Moreover, most (~90%) of the energy necessary for the interaction with the TCR is peptide independent and is given solely by the major histocompatibility complex (MHC) molecule. The peptide turns this initial association into stable binding, thus imparting specificity and eliciting T-cell activation by modulating the duration of the contact (2).

T-cell activation in response to signals through the TCR range from proinflammatory responses to anergy and apoptosis, outcomes that reflect normal mechanisms of peripheral tolerance (1). Studies of the TCR signaling pathways primarily take advantage of monoclonal antibodies (mAbs) to the CD3 to supply a surrogate signal in place of the MHC peptide complex presented by antigen-presenting cells (APCs) (3). Several features limit the fidelity of these systems: *1*) the affinity of mAb binding is higher than that of MHC class II/TCR interactions, *2*) anti-CD3 stimulation does not depend on recognition by the TCR of the processed antigen in the MHC class II groove, and *3*) there is no CD4 engagement (4). These issues are particularly relevant in studies of autoimmune reactivity, where TCR/MHC interactions of low affinity occur. An alternative approach is to use soluble recombinant MHC molecules, multivalently complexed to gain higher avidity and to mimic the APC display. MHC class II oligomers are capable of eliciting T-cell activation responses when used to bind the TCR on mouse (4–7) and human (8–11) antigen-specific T-cell clones. In our studies, human MHC class II tetramers (TMrs) have been used to detect, isolate, and characterize epitope-specific CD4$^+$ T-cells associated with viral infections (8,9,12) and with autoimmunity against the GAD65 immunodominant antigen of type 1 diabetes (13). In the latter study, in vitro antigen-specific expansion and TMr analysis identified low-avidity low-frequency autoreactive CD4$^+$ T-cells with DR4-restricted GAD specificity in type 1 diabetic subjects. We now use GAD-reactive T-cells with different TCR avidities to characterize activation parameters and thresholds for self-antigen recognition, using human class II TMrs as ligands for the TCR.

RESEARCH DESIGN AND METHODS

HLA-DR0401 TMrs. The construction of the expression vectors used to generate soluble HLA-DR0401 molecules has been described elsewhere (8). Briefly, chimeric cDNA was generated from the extracellular coding regions of the DRB1*0401 and DRA1*0101 chains attached to leucine zipper motifs followed by a site-specific biotinylation sequence on the DRβ chain. These cDNAs were subcloned into Cu^{2+}-inducible *Drosophila* expression vectors, followed by cotransfection into Schneider S-2 cells. The assembled soluble MHC class II molecules were subsequently purified, biotinylated, and loaded with peptides (5:1 peptide/MHC molar ratio) at pH 6.0. The type 1 diabetes GAD65 555–567 immunodominant epitope (NFFRMVISNPAAT) was used as a cognate peptide. A 557I substitution enhancing its agonistic activity (14) was necessary to achieve sufficient T-cell yields after in vitro antigen-specific expansion (13). Irrelevant control peptides were as follows: myelin basic protein (MBP) 83–99 (ENPVVHFFKNIVTPRTP), *B. burgdorferi* outer surface protein A 163–175 (KSYVLEGTLTAEK), and influenza A hemagglutinin 306–318 (KYVKQNTLKLA). All the peptides used bind to the soluble DR0401 MHC

From the [1]Benaroya Research Institute at Virginia Mason, Seattle, Washington; and the [2]Department of Immunology, University of Washington School of Medicine, Seattle, Washington.

Address correspondence and reprint requests to Gerald T. Nepom, MD, PhD, Benaroya Research Institute at Virginia Mason, 1201 Ninth Ave., Seattle, WA 98101-2795. E-mail: nepom@benaroyaresearch.org.

Received for publication 27 August 2003 and accepted in revised form 8 January 2004.

AICD, activation-induced cell death; ann-V, annexin V; APC, antigen-presenting cell; CFSE, carboxyfluorescein diacetate succinimidyl ester; IFN, interferon; IL, interleukin; mAb, monoclonal antibody; MBP, myelin basic protein; MHC, major histocompatibility complex; PBMC, peripheral blood mononuclear cell; PE, phycoerythrin; PLC, phospholipase C; sFasL, soluble Fas ligand; TCR, T-cell receptor; TMr, tetramer.

molecule with similar affinities, as assessed in MHC binding competition assays. TMrs were obtained by coupling DR0401 molecules with phycoerythrin (PE)-labeled streptavidin at a molar ratio of 8:1. Irrelevant DR1501 TMrs were similarly produced and used as additional controls.

T-cell clones. Peripheral blood mononuclear cells (PBMCs) from an HLA-DR0401$^+$ type 1 diabetic patient were stimulated as described earlier (13). Briefly, PBMCs were cultured in the presence of 10 μg/ml GAD peptide for 10 days and subsequently transferred onto wells that had been absorbed with 8 μg/ml GAD-loaded DR0401 monomer. On day 5, cells were stained with PE-labeled GAD-loaded TMr (TMr-GAD) and fluorochrome-labeled anti-CD25 and anti-CD4 mAbs (PharMingen, San Diego, CA). After washing, CD4$^+$CD25$^+$ TMr-GAD$^+$ cells were single-cell sorted using a FACSVantage cell sorter (BD Immunocytometry Systems, San Jose, CA). Clones thus obtained were expanded for 13 days by stimulation with irradiated unmatched PBMCs, phytohemagglutinin (5 μg/ml; Sigma, St. Louis, MO) and interleukin (IL)-2 (10 units/ml; Chiron, Emeryville, CA) for two rounds. Cells were subsequently stimulated with HLA-DR0401$^+$ PBMCs pulsed with 10 μg/ml GAD peptide and 10 units/ml IL-2 and selected by growth on day 14 for further expansion. One hundred clones were tested for TMr-GAD staining: 20 TMr-GAD$^+$ clones were selected and further tested for [^{3}H]-TdR incorporation after stimulation with irradiated autologous PBMCs with and without GAD peptide. All 20 clones displayed TCR Vα12 Vβ5.1 rearrangement and identical TCR sequences.

Clones BRI4.1 and BRI4.13 were chosen for further study. They displayed similar TCR and CD4 expression, similar T helper memory phenotypes (i.e., CD3$^+$CD4$^+$CD45RO$^+$CD45RB^{low}CD44^{high}CD27$^-$CD11a^{high}), and similar Th0 patterns of cytokine secretion (i.e., interferon [IFN]-γ, IL-4, IL-5, and IL-10) after APC stimulation, although the most abundant cytokine produced was IL-5 for the BRI4.1 and IFN-γ for the BRI4.13 clone. Clones were maintained by stimulation at 2-week intervals with either irradiated non–HLA-matched PBMCs, phytohemagglutinin and IL-2, or GAD peptide–pulsed DR0401$^+$ PBMCs and IL-2. Cells were used at days 11–15 after stimulation in all experiments; proliferation studies were carried out at day 6 to take advantage of the full proliferative potential.

All experiments were performed at least in duplicate and are depicted as means ± SE. All figures are representative of the results from at least two independent experiments.

Quantitative flow cytometry. Cells were incubated for 3 h at 37°C in the presence of TMrs and subsequently washed twice in PBS containing 0.1% fetal bovine serum and 0.01% NaN_3. A BD FACSCalibur flow cytometer was calibrated with QuantiBRITE PE beads (BD Immunocytometry Systems), containing known amounts of PE molecules. The calibration curve thus obtained was used to estimate the number of molecules of PE-labeled reagent bound per cell from the median fluorescence intensity of the samples.

Ca^{2+} mobilization. Five million cells were washed twice in PBS and loaded with 4 μmol/l Fluo-3 AM (Molecular Probes, Eugene, OR) in the presence of 0.01% Pluronic F127 for 1 h at 37°C (15). Cells were then washed three times in Fluo-3 buffer (137 mmol/l NaCl, 5 mmol/l KCl, 1 mmol/l Na_2HPO_4, 5 mmol/l glucose, 1 mmol/l $CaCl_2$, 0.5 mmol/l $MgCl_2$, 1 g/l BSA, and 10 mmol/l HEPES, pH 7.4), resuspended in the same medium at a concentration of 10^6 cells/ml, and kept at 37°C for the whole duration of measurements. Sample aliquots were analyzed by flow cytometry every 2 min, acquiring ~2,000 events during a 5-s fixed-time reading. After assessment of the basal fluorescence level at two different time points (−4 and −2 min), relevant stimuli were added (0 min) and the readings continued for a total of 30 min. UCHT-1 anti-CD3 mAb (10 μg/ml; PharMingen) cross-linked with a fourfold concentration of rabbit polyclonal anti-mouse IgG (Jackson ImmunoResearch, West Grove, PA) was used as a positive control.

Phospholipase C-γ_1 phosphorylation. Cells were starved overnight in RPMI containing 0.5% pooled human serum, washed in ice-cold RPMI, and rested for 30 min on ice. GAD- or MBP-loaded TMr (60 μg/ml), cross-linked anti-CD3 mAb (30 μg/ml), or PBS was added on ice, and cells were subsequently stimulated at 37°C for the indicated time. The reaction was stopped by adding an equal volume of 1% NP-40 lysis buffer (15). Lysates were boiled in SDS-reducing sample buffer, run on 8% SDS-PAGE, and transferred onto polyvinylidene difluoride membranes. After blocking, blots were probed with horseradish peroxidase–conjugated PY20 anti-phosphotyrosine mAb (Santa Cruz Biotechnology, Santa Cruz, CA) and developed with enhanced chemiluminescence reagents (Amersham, Piscataway, NJ). Membranes were then stripped in 150 mmol/l NaCl and 10 mmol/l Tris-HCl (pH 2.2), blocked, and reprobed with C37 anti–phospholipase C (PLC)-γ_1 rabbit serum (a gift from Dr. J. Sancho, CSI, Granada, Spain) to confirm equal loading of lanes (15).

CD69 upregulation. T-cells were incubated for 3 h at 37°C with either GAD-loaded DR0401 TMr (TMr-GAD) or with the same TMr loaded with irrelevant peptides at the indicated concentrations. Cells were then washed in PBS containing 0.1% fetal bovine serum and 0.01% NaN_3, stained with an allophycocyanin-labeled anti-CD69 mAb (PharMingen), and analyzed by flow cytometry.

Real-time PCR for cytokine mRNA. Cells were stimulated with TMrs (10 μg/ml) for 6 h, and RNA was extracted using an RNeasy kit (Qiagen, Valencia, CA). cDNA was prepared using random hexamers (2.5 μmol/l). Message levels were quantified by real-time PCR using the ABI 7000 Sequence Detection System (Applied Biosystems). Primers were designed so that amplicons spanned intron/exon boundaries to minimize amplification of genomic DNA. Primer sequences were as follows: GAPDH, 5′-CCACATCGCTCAGACACCAT-3′ and 5′-GGCAACAATATCCACTTTACCAGAGT-3′; IFN-γ, 5′-GCTGTTACTGCCAGGACCCATA-3′ and 5′-TCACTCTCCTCTTTCCAATTCTTCA-3′; tumor necrosis factor-α, 5′-TCTCGAACCCCGAGTGACA-3′ and 5′-GGCCCGGCGGTTCA-3′; IL-2, 5′-AAGAATCCCAAACTCACCAGGAT-3′ and 5′-TCTAGACACTGAAGATGTTTCAGTTCTG-3′; IL-4, 5′-CGACTGCACAGCAGTTCCA-3′ and 5′-CTCTGGTTGGCTTCCTTCACA-3′; IL-5, 5′-GAAAGAGACCTTGGCACTGCTT-3′ and 5′-AGTGTGCCTATTCCCTGAAAGATT-3′; and IL-10, 5′-GAGGCTACGGCGCTGTCA-3′ and 5′-CTTGGAGCTTATTAAAGGCATTCTTC-3′. Amplification was carried out in a total volume of 25 μl for 40 cycles of 15 s at 95°C and 1 min at 60°C. Products were detected using SYBR Green I dye (Molecular Probes). Samples were run in triplicate, and their relative mRNA levels were determined by normalizing expression of each gene to GAPDH. The normalized values of unstimulated samples were then compared with those of TMr-MBP– and TMr-GAD–treated cells to calculate mRNA fold changes.

Cytokine secretion and proliferation. Cells (10^5/well) were cultured in triplicate in 96-well round-bottom plates with different TMr concentrations for 36 h, after which 50 μl of supernatant was removed from each well and analyzed for cytokines using a cytometric bead array system (BD Immunocytometry Systems). [^{3}H]-TdR was added (1 μCi/well), and cells were cultured for an additional 24 h, harvested, and their incorporation determined using a Wallac liquid scintillation β-counter (Perkin-Elmer, Shelton, CT).

Apoptosis. Cells were cultured for 12 h at different TMr concentrations, as indicated. After washing in cold annexin V (ann-V) binding buffer (140 mmol/l NaCl, 10 mmol/l HEPES, 2.5 mmol/l $CaCl_2$, pH 7.4), cells were stained for 20 min on ice with fluorescein isothiocyanate–conjugated ann-V (PharMingen) along with 1 μg/ml 7-amino actinomycin D (Sigma). In selected experiments, GM6001 matrix metalloproteinase inhibitor (15 μmol/l; Chemicon, Temecula, CA), neutralizing anti-Fas ligand mAb (20 μg/ml; PharMingen), or control IgG was added with the TMrs, as indicated. Soluble Fas ligand (sFasL) released in the culture supernatants was measured by ELISA (Immunotech/Beckman Coulter, Miami, FL). To correlate apoptotic and proliferative events, cells were labeled in 0.8 μmol/l carboxyfluorescein diacetate succinimidyl ester (CFSE) (Molecular Probes) for 8 min at 37°C, washed, plated as above, and cultured for 48 h at a 5 μg/ml TMr concentration. After harvesting, cells were washed in ann-V binding buffer, stained with Cy5-labeled ann-V (PharMingen), and analyzed by flow cytometry.

RESULTS

TMr-GAD binds to a limited number of TCRs. The number of TCRs bound at each TMr concentration was measured by quantitative flow cytometry. Based on the tetrahedrical configuration of streptavidin (16), we assumed average engagement of three TCR molecules per TMr bound. When the GAD-specific BRI4.1 and BRI4.13 T-cell clones were incubated with high concentrations (20 μg/ml) of DR0401 TMr loaded with the same GAD peptide (TMr-GAD), only 6.7–11.5% of the TCRs available (as estimated by PE-labeled anti-CD3 mAb binding) were occupied (Fig. 1). This figure gradually decreased with lower TMr-GAD concentrations, reaching levels more than 10-fold lower (299 ± 75 TMr-bound TCRs per cell; 0.4–0.6%) at 0.3 μg/ml. Clone BRI4.1 displayed lower avidity than clone BRI4.13. On the contrary, the same DR0401 TMr loaded with MBP 83–99 (TMr-MBP) as well as with other irrelevant peptides did not show any significant binding throughout the concentration range.

Early activation events: both TMr-GAD and irrelevant TMrs induce Ca^{2+} mobilization and PLC-γ_1 phosphorylation. The initiation of TMr-induced signal transduction was followed by real-time Ca^{2+} measurements on the BRI4.13 clone (Fig. 2). At a TMr-GAD

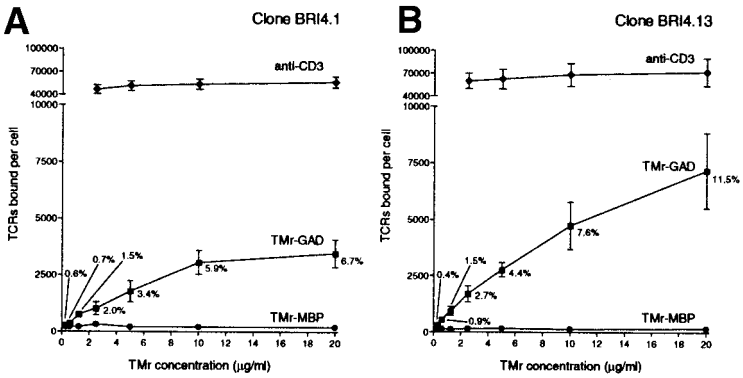

FIG. 1. MHC class II TMr binding to TCR. BRI4.1 (*A*) and BRI4.13 (*B*) T-cells were incubated with GAD- or MBP-loaded DR0401 TMr or anti-CD3 mAb for 3 h at 37°C. The number of TCRs bound per cell was derived by comparing the number of molecules of PE-labeled reagents with a calibration curve obtained with beads containing known amounts of PE molecules. The percent number of TCRs bound by TMr-GAD out of the total TCRs available (as estimated from anti-CD3 mAb binding) is also shown.

concentration of 20 μg/ml (Fig. 2*A*), the intracellular Ca^{2+} concentration started rising as early as 2–4 min after addition of the TMr and increased gradually until reaching its maximum at 10 min, followed by a similarly gradual decrease to the basal level by 24 min. A smaller and slow-onset increase in Ca^{2+} fluxes was registered with the MBP-loaded TMr (Fig. 2*A*), as well as with TMrs loaded with outer surface protein A and hemagglutinin irrelevant DR0401-binding peptides, whereas no signal was triggered by an irrelevant DR1501 TMr (data not shown).

The effect was dose dependent (Fig. 2*B* and *C*) and was still observed at concentrations as low as 2.5 μg/ml, where the TMr-GAD–induced Ca^{2+} signal was lower in amplitude as well as delayed in onset, whereas the signal obtained with TMr-MBP became negligible. Anti-CD3 stimulation (10 μg/ml) led to an extremely fast Ca^{2+} response, peaking at 2 min (Fig. 2*D*), consistent with the much higher affinity of antigen/mAb interactions as well as with the higher avidity obtained by cross-linking. No signal was detected with an irrelevant isotype-matched IgG.

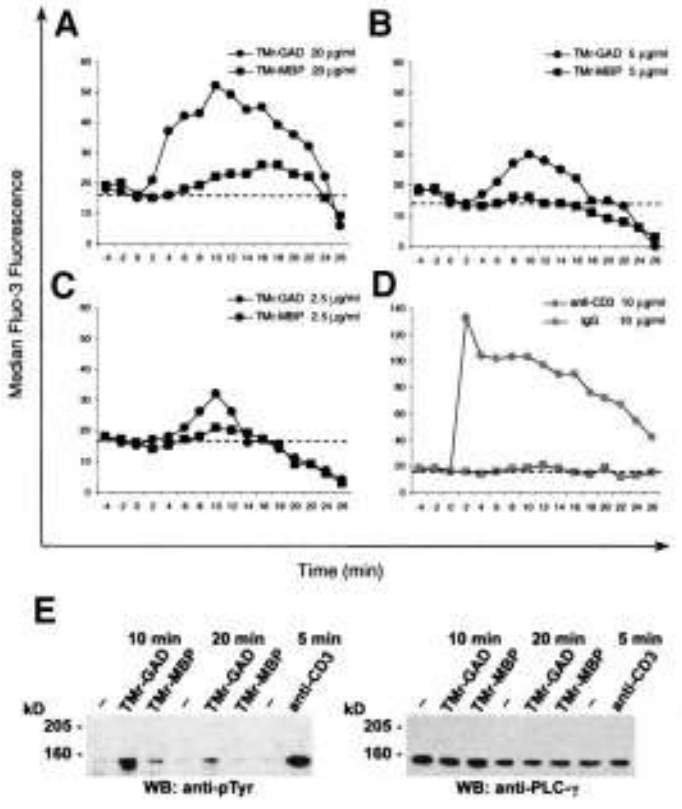

FIG. 2. Ca^{2+} mobilization and PLC-γ_1 phosphorylation upon TMr stimulation. *A–D*: Cells were loaded with the Ca^{2+}-sensitive fluorescent dye Fluo-3 AM and kept at 37°C, and their median fluorescence was measured every 2 min before and after the addition ($t = 0$) of the indicated stimuli. The dotted lines in each graph indicate the basal Ca^{2+} level before stimulation. *E*: Cells were incubated with TMr-GAD, TMr-MBP, or anti-CD3 mAb and stimulated at 37°C for the indicated time. Lysates were probed with anti-phosphotyrosine mAb (*left*) and subsequently with the specific anti– PLC-γ_1 antibody (*right*) in Western blot (WB).

Ca^{2+} mobilization was accompanied by PLC-γ_1 phosphorylation (Fig. 2*E*). As suggested by the Ca^{2+} profiles, the different on-rate kinetics of TMrs and mAbs required different time frames for the two reagents. PLC-γ_1 phosphorylation was strongly induced at 10 min and still maintained at 20 min by TMr-GAD (Fig. 2*E*, *left*). TMr-MBP was capable of delivering a low-level transient signal, readily detectable after 10 min but already quenched at 20 min. Cross-linked anti-CD3 mAb induced consistent phosphorylation after 5 min. Reprobing the membrane with the specific anti–PLC-γ_1 antibody confirmed the identity of the highlighted bands (Fig. 2*E*, *right*).

Late activation events: TMr-GAD but not irrelevant TMrs induces CD69 upregulation. Phosphorylation and Ca^{2+} signal transduction cascades ultimately lead to the formation of active transcription factor complexes, which initiate the expression of new genes. The earliest of the newly synthesized surface proteins, detectable after complete T-cell activation, is CD69 (17). CD69 was readily induced on the cell surface by TMr-GAD stimulation for 3 h. Different basal levels of CD69 expression did not allow for reliable comparison of clones BRI4.1 and BRI4.13; results for clone BRI4.13 are shown in Fig. 3. The upregulating effect on CD69 was dose dependent and reached saturation at a TMr-GAD concentration of 10 μg/ml. The minimal effective concentration was 0.3 μg/ml, compared with the almost 10-fold higher 2.5 μg/ml minimal concentration required for Ca^{2+} mobilization. This reflects the Ca^{2+} signal requirement for high TMr-GAD concentrations to overcome the slow on-rate and fast off-rate of MHC-TCR interactions (9), whereas fast TCR occupancy is not a requirement for the slow-onset CD69 induction. In contrast to early signal transduction events, T-cells treated with TMr-MBP (10 μg/ml) as well as with TMrs loaded with other irrelevant peptides did not show significant CD69 upregulation. An effect similar to the one induced by TMr-GAD was observed with the anti-CD3 mAb–positive control, whereas no upregulation was triggered by an isotype-matched IgG.

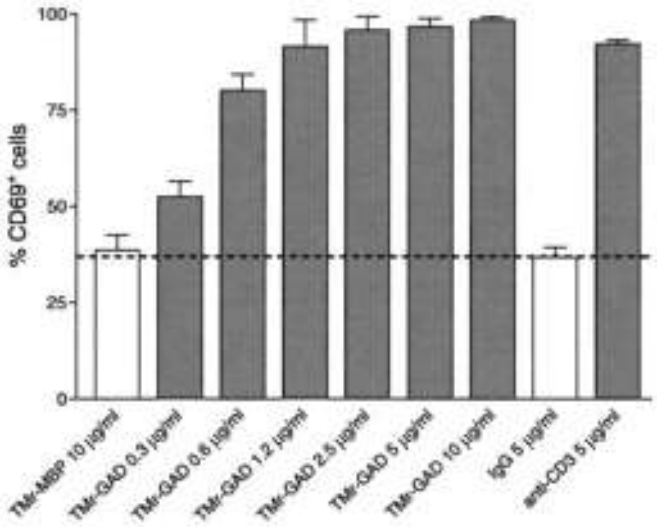

FIG. 3. CD69 upregulation by MHC class II TMr-GAD. Cells were stimulated with irrelevant TMr-MBP or IgG (□) or with TMr-GAD or anti-CD3 mAb (■) at the indicated concentrations for 3 h at 37°C. The dotted line shows the basal CD69 expression in unstimulated cells.

Late activation events: cytokine mRNA transcription and protein secretion are specifically induced by TMr-GAD. Besides CD69 expression, other complex activation events requiring mRNA transcription and new protein synthesis were elicited by TMr-GAD, but not by TMrs loaded with irrelevant peptides. First, we looked at the induction of mRNA transcription for Th1 and Th2 cytokines after TMr stimulation. As shown in Fig. 4*A*, TMr-GAD but not TMr-MBP (both used at the optimal concentration of 10 μg/ml) specifically induced cytokine mRNAs in BRI4.13 cells after a 6-h stimulation. These

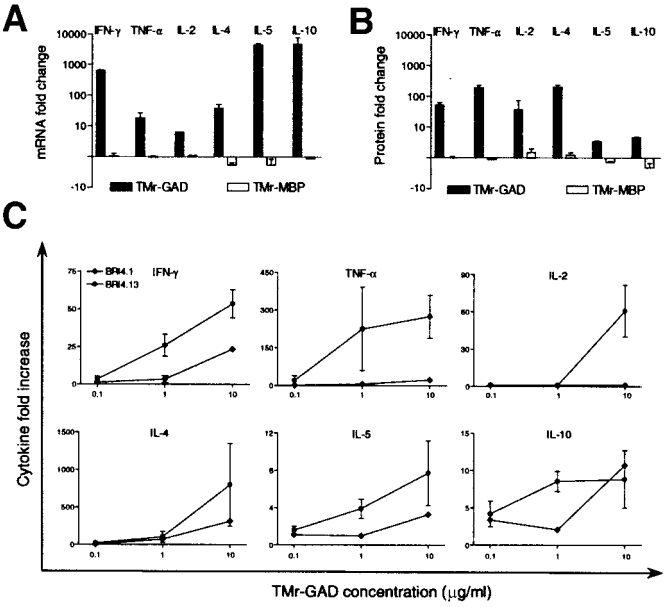

FIG. 4. Cytokine mRNA and protein induction by MHC class II TMr-GAD. *A*: Cells were stimulated with 10 μg/ml TMr-GAD (■) or TMr-MBP (□) for 6 h at 37°C, and the specific mRNA levels were measured by real-time PCR. *B*: Cells were stimulated with 10 μg/ml TMrs for 36 h at 37°C, and the specific cytokines were measured in culture supernatants. Fold changes are shown in a $\log_{10}$ scale. *C*: BRI4.1 (♦) and BRI4.13 (●) clones were cultured with TMr-GAD (0.1–1-10 μg/ml) for 36 h, and the indicated cytokines were measured in culture supernatants.

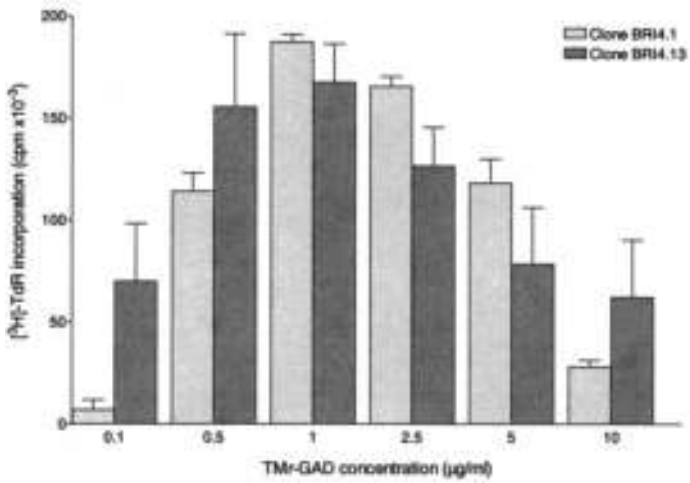

FIG. 5. TMr-GAD–induced proliferation of BRI4.1 and BRI4.13 clones. Cells were cultured with TMr-GAD at the indicated concentrations for 60 h, and [^{3}H]-TdR was added for the last 24 h.

TMr-GAD–specific transcriptional changes were also evident when the final protein products were analyzed after 36 h of stimulation (Fig. 4*B*). Higher TMr-GAD concentrations achieved higher cytokine secretion (Fig. 4*C*). Moreover, the BRI4.1 lower-avidity clone displayed a lower sensitivity to stimulation than the BRI4.13 higher-avidity clone for all the cytokines evaluated (Fig. 4*C*).

TMr-GAD–activated T-cells undergo proliferation and subsequent activation-induced cell death. When the proliferative response to TMr stimulation was analyzed by [^{3}H]-TdR incorporation (Fig. 5), the dose dependency observed for the other effects was maintained only up to 1 μg/ml TMr-GAD; a further increase in TMr-GAD concentration (≥2.5 μg/ml) gave a dose-dependent decrease in response. Moreover, the BRI4.1 lower-avidity clone displayed the expected lower sensitivity only at the low–TMr-GAD concentrations, whereas its proliferative response was even higher than that of BRI4.13 in the 1–5 μg/ml range. No proliferative response was observed with TMr-MBP.

The bell-shaped curve of TMr-GAD–induced proliferation suggested that not only cell division, but also apoptosis, could be triggered at high concentrations. Indeed, decreased [^{3}H]-TdR incorporations do not discriminate between growth arrest and cell death (18). To verify this hypothesis, BRI4.13 cells were cultured for 12 h in the presence of different stimuli, stained with ann-V, and compared to basal unstimulated conditions. As shown in Fig. 6*A*, a marginal proportion (7%) of apoptotic (ann-V$^+$) cells accumulated with TMr-GAD concentrations up to 1 μg/ml, i.e., the dose at which maximal [^{3}H]-TdR incorporation was observed (Fig. 5). However, the apoptotic fraction significantly increased from concentrations as low as 2.5 μg/ml (Fig. 6*B*). The effect was dose dependent, with a 58% maximal increase at 10 μg/ml (Fig. 6*C*). The apoptosis induced by irrelevant TMrs such as TMr-MBP, used at the optimal 10 μg/ml concentration, was negligible (Fig. 6*D*). The pro-apoptotic effect at the optimal TMr-GAD concentration was of such magnitude to be readily detectable by morphological parameters (Fig. 6*E*). The BRI4.1 lower-avidity clone displayed lower susceptibility to cell death, as evidenced by the limited accumulation of apo-

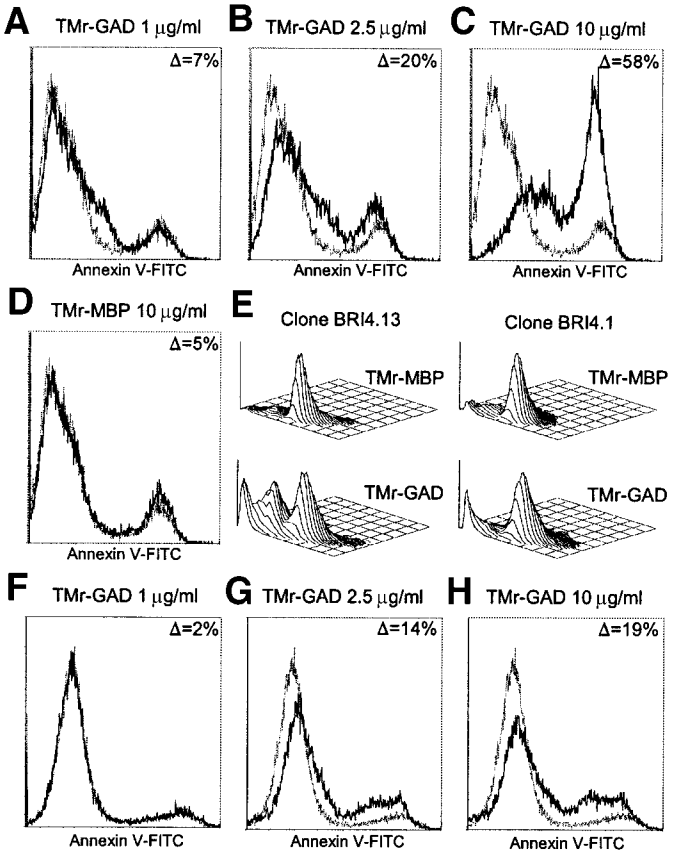

FIG. 6. TMr-GAD–induced apoptosis of T-cells. Cells were cultured for 12 h in the presence of TMrs at the indicated concentrations. *A–D*: Histograms show the ann-V staining of stimulated cells (solid lines) and the percent increase in apoptotic (ann-V$^+$) cells compared with the basal unstimulated condition (dotted lines) for the BRI4.13 (*A–D*) and BRI4.1 (*F–H*) clones. *E*: Three-dimensional plots of forward and side scatter distribution among TMr-MBP– and TMr-GAD–treated BRI4.13 and BRI4.1 clones. FITC, fluorescein isothiocyanate.

ptotic bodies in three-dimensional plots (Fig. 6*E*) as well as by the different dose-dependent titration of the effect (Fig. 6*F–H*).

The observed apoptotic events were characteristic of activation-induced cell death (AICD). Consistent with the notion that AICD is mainly mediated by the Fas/FasL death receptor system (19), TMr-GAD–induced apoptosis was accompanied by a dose-dependent release of sFasL in the BRI4.13 cell culture supernatants (Fig. 7*A*), whereas no detectable sFasL (<0.1 ng/ml) was released by the BRI4.1 clone, nor was it released by either clone treated with TMr-MBP (data not shown). Furthermore, TMr-GAD–induced apoptosis was *1*) inhibited by decreasing the Fas/FasL interaction by means of a neutralizing anti-FasL mAb (Fig. 7*B*) and *2*) enhanced by increasing the Fas/FasL interaction with a matrix metalloproteinase inhibitor blocking the release of surface FasL into the soluble form (Fig. 7*C*); indeed, this potentiation of apoptosis correlated with the increase in surface FasL expression (Fig. 7*D*).

The apparent paradox between the proliferative and apoptotic effects of TMr-GAD stimulation was further clarified by CFSE/ann-V double staining (Fig. 8). As compared with TMr-MBP–treated cells, a significant fraction of TMr-GAD–stimulated cells (5 μg/ml, 48 h) underwent both apoptosis, turning ann-V$^+$, and an appreciable number of

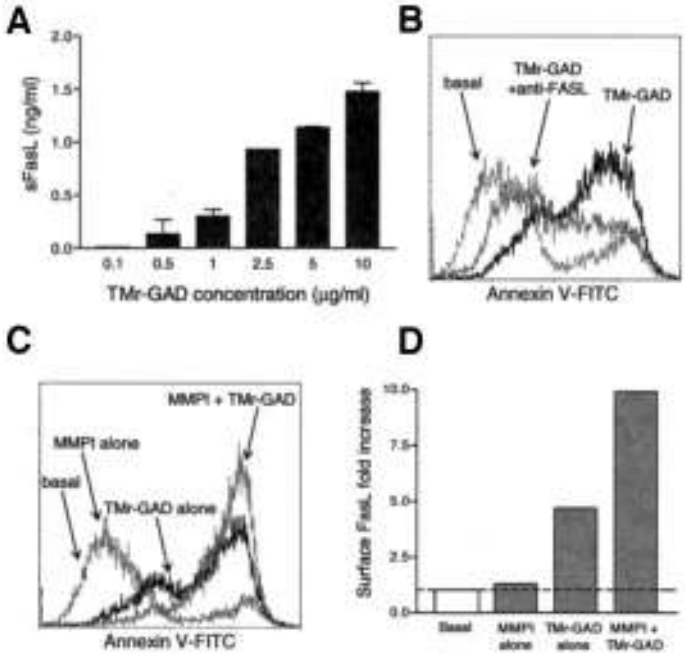

FIG. 7. The apoptotic effect of TMr-GAD (10 μg/ml, 12 h) is due to activation-induced cell death. *A*: Dose-dependent release of sFasL by TMr-GAD–treated BRI4.13 cells, as measured by ELISA. *B*: Inhibition of TMr-GAD–induced apoptosis by a blocking anti-FasL mAb. *C*: Potentiation of TMr-GAD–induced apoptosis by a matrix metalloproteinase inhibitor (MMPI) blocking the release of sFasL. *D*: Concomitant increase in surface FasL expression. FITC, fluorescein isothiocyanate.

cell divisions, as reflected by the decrease in CFSE staining. Progression into the cell cycle is a prerequisite for AICD (20), and the cells that had divided (CFSE^{low}) preferentially underwent apoptosis, as shown by the presence of two major populations of TMr-GAD–treated cells, CFSE^{high}ann-V$^-$ (undivided, viable) and CFSE^{low}ann-V$^+$ (divided, apoptotic). On the contrary, TMr-MBP–stimulated cells underwent negligible apoptosis as well as marginal proliferation, and the majority of cells remained in the CFSE^{high}ann-V$^-$ quadrant, i.e., they were still undivided and viable.

DISCUSSION

MHC class II TMr stimulation provides a faithful representation of T-cell activation. Consistent with the potent TCR signal delivered, no costimulation was necessary (6,21). Although a substituted GAD peptide was required to achieve sufficient in vitro expansion of peripheral blood

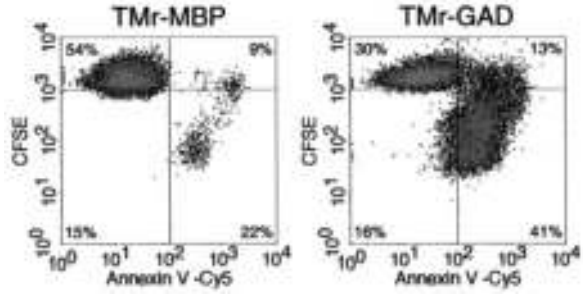

FIG. 8. Correlation between proliferative and apoptotic events in T-cells stimulated for 48 h with 5 μg/ml TMr-GAD or TMr-MBP. Density plots show double ann-V and CFSE staining. The percent of cells in each plot quadrant is indicated.

$CD4^+$ T-cells (13), the stimulatory potency of TMrs is of note considering the nonsaturating binding of MHC class II TMrs, which occupied only a small fraction of the TCRs available. Two hundred to 300 interactions have been described as the minimal TCR signaling requirement in T-cell/APC contact models (22), numbers similar to the estimate of the TMr-binding sites at the minimal effective concentrations of 0.25–0.5 μg/ml. The potent signals delivered by MHC class II TMrs despite binding to so few TCRs could be partly explained by a serial engagement model (23). This model proposes that a few hundred specific peptide/MHC complexes on the surface of an APC are capable of mediating the specific downregulation of many thousands of TCRs on a T-cell by transient serial binding events. Similarly, each single MHC arm within the TMr could transiently contact and scan a large number of TCRs by serial fast interactions. At the same time, the TMr as a whole would be kept bound to the cell surface by the overall avidity of the complex.

The T-cell can be viewed as a signal integrator, in which the number of interactions and duration of each contact set varying thresholds for activation. TCR interactions with the peptide mainly influence the off-rate of binding, but not the on-rate; in this two-step process of TCR recognition, the TCR-MHC contacts are permissive for signaling, whereas the TCR peptide contacts are required for sustained outcomes (2). Nonetheless, transient MHC-directed TCR engagements are important contributors to effective signaling and antigen sensitivity (24). Moreover, Davis and colleagues (25,26) noted the participation of "nonspecific" endogenous peptide–MHC-TCR interactions in the complete formation of the immunological synapse. Another important context for subthreshold signals through MHC-TCR interactions is homeostasis (27), representing an in vivo control mechanism of T-cell survival. MHC class II TMrs offer a novel approach to address these issues, allowing to follow both the peptide–MHC-TCR binding and the signaling events in an APC-free system. Indeed, TMrs loaded with irrelevant peptides did not bind the TCR but were nonetheless capable of some degree of early signal transduction. This reflects fast, transient TMr/TCR interactions, which are capable of early signaling but are not followed by stable TMr binding and signal progression. Indeed, the low-level early signals delivered by noncognate TMrs were not mirrored by late activation events. In this context, function of the GAD peptide in the MHC groove would be to stabilize transient contacts (2), allowing more efficient progression of the signal and subsequent full activation. The two-step model of TCR recognition is consistent with our interpretation of the TCR/noncognate TMr interaction, which corresponds to the initial permissive contact but lacks sustained signaling.

So far, preliminary in vitro antigen-specific expansion has proven unavoidable to visualize autoreactive $CD4^+$ T-cells in different autoimmune diseases (13,28,29). With this limitation, another major novelty of the present study is the analysis of TCR recognition and activation requirements in the autoimmune context of human diabetes. TMr activation of self-antigen–reactive T-cells from a diabetic patient indicates that immune response profiles follow a gradient of response. This gradient shows an overlapping strength of signal-eliciting proliferation and cytokine release, a measure of proinflammatory activation, as well as AICD, a measure of regulated apoptosis (30). The direct relationship between proliferation and apoptosis at the single-cell level has been previously demonstrated in superantigen-induced AICD (31). The similar correlation upon antigen-specific stimulation found in our study reinforces the notion that these two T-cell outcomes are finely balanced by subtle quantitative differences to provide a key control mechanism of normal and aberrant immunological responses (32).

The fact that two T-cell clones harboring the same TCR displayed different strengths of TMr interaction is of interest and could be related to differences in membrane fluidity or TCR clustering (33). The lower structural avidity (TMr-GAD binding) of the BRI4.1 clone was paralleled by a lower functional avidity (TMr-GAD signaling). This lower sensitivity to activation endowed this clone with relative resistance to AICD. This suggests that low-avidity autoreactive T-cells might have a survival advantage over high-avidity T-cells and could thus be important contributors in chronic autoimmune pathology.

TMrs containing autoantigen peptides have clinical utility in autoimmunity for diagnostic and, potentially, therapeutic applications. Results from the first clinical trial using a nonactivating humanized form of OKT3 anti-CD3 mAb in new-onset type 1 diabetes showed a consistent, although transient, improvement in β-cell function (34). In these respects, MHC class II multimers could represent an appealing therapeutic alternative to OKT3, endowed with better specificity and acting by different mechanisms, including the induction of apoptosis, as shown in our model, and/or anergy, as observed in murine (35) and human (21) systems with MHC class II dimers. However, high-avidity T-cells would be preferentially targeted, whereas potentially relevant low-avidity clones would be relatively spared. The selective nature of this approach requires knowledge of the relevant immunodominant epitopes, which likely involve other autoantigens besides GAD. It may also require intervention early in the disease process, before extensive epitope spreading has occurred. In this respect, "immune staging" protocols with periodic screening of pre-diabetic individuals with the same TMrs may allow to select the best candidates for specific immunomodulatory intervention. Disappointing results with antigen-based therapeutics (36) underline the necessity to better understand the properties of MHC-based reagents that facilitate the desired tolerization outcome.

ACKNOWLEDGMENTS

This work was supported in part by the Juvenile Diabetes Research Foundation International and by grant DK 53004 from the National Institutes of Health.

We gratefully acknowledge Dr. G. Baj for helping set up the calcium measurement method. R.M. is student at the Postgraduate School of Internal Medicine, University of Turin, Turin, Italy.

This work is dedicated to the memory of Sperato Mallone.

REFERENCES

1. Anderton SM, Wraith DC: Selection and fine-tuning of the autoimmune T-cell repertoire. *Nat Rev Immunol* 2:487–498, 2002
2. Wu LC, Tuot DS, Lyons DS, Garcia KC, Davis MM: Two-step binding

mechanism for T-cell receptor recognition of peptide MHC. *Nature* 418: 552–556, 2002
3. Unanue ER: Perspective on antigen processing and presentation. *Immunol Rev* 185:86–102, 2002
4. Hamad AR, O'Herrin SM, Lebowitz MS, Srikrishnan A, Bieler J, Schneck J, Pardoll D: Potent T cell activation with dimeric peptide-major histocompatibility complex class II ligand: the role of CD4 coreceptor. *J Exp Med* 188:1633–1640, 1998
5. Crawford F, Kozono H, White J, Marrack P, Kappler J: Detection of antigen-specific T cells with multivalent soluble class II MHC covalent peptide complexes. *Immunity* 8:675–682, 1998
6. Boniface JJ, Rabinowitz JD, Wulfing C, Hampl J, Reich Z, Altman JD, Kantor RM, Beeson C, McConnell HM, Davis MM: Initiation of signal transduction through the T cell receptor requires the multivalent engagement of peptide/MHC ligands. *Immunity* 9:459–466, 1998
7. Casares S, Zong CS, Radu DL, Miller A, Bona CA, Brumeanu TD: Antigen-specific signaling by a soluble, dimeric peptide/major histocompatibility complex class II/Fc chimera leading to T helper cell type 2 differentiation. *J Exp Med* 190:543–553, 1999
8. Novak EJ, Liu AW, Nepom GT, Kwok WW: MHC class II tetramers identify peptide-specific human CD4(+) T cells proliferating in response to influenza A antigen. *J Clin Invest* 104:R63–R67, 1999
9. Reichstetter S, Ettinger RA, Liu AW, Gebe JA, Nepom GT, Kwok WW: Distinct T cell interactions with HLA class II tetramers characterize a spectrum of TCR affinities in the human antigen-specific T cell response. *J Immunol* 165:6994–6998, 2000
10. Cochran JR, Cameron TO, Stern LJ: The relationship of MHC-peptide binding and T cell activation probed using chemically defined MHC class II oligomers. *Immunity* 12:241–250, 2000
11. Appel H, Gauthier L, Pyrdol J, Wucherpfennig KW: Kinetics of T-cell receptor binding by bivalent HLA-DR: peptide complexes that activate antigen-specific human T-cells. *J Biol Chem* 275:312–321, 2000
12. Novak EJ, Masewicz SA, Liu AW, Lernmark A, Kwok WW, Nepom GT: Activated human epitope-specific T cells identified by class II tetramers reside within a CD4 high, proliferating subset. *Int Immunol* 13:799–806, 2001
13. Reijonen H, Novak EJ, Kochik S, Heninger A, Liu AW, Kwok WW, Nepom GT: Detection of GAD65-specific T-cells by major histocompatibility complex class II tetramers in type 1 diabetic patients and at-risk subjects. *Diabetes* 51:1375–1382, 2002
14. Masewicz SA, Papadopoulos GK, Swanson E, Moriarity L, Moustakas AK, Nepom GT: Modulation of T cell response to hGAD65 peptide epitopes. *Tissue Antigens* 59:101–112, 2002
15. Mallone R, Funaro A, Zubiaur M, Baj G, Ausiello CM, Tacchetti C, Sancho J, Grossi C, Malavasi F: Signaling through CD38 induces NK cell activation. *Int Immunol* 13:397–409, 2001
16. McMichael AJ, O'Callaghan CA: A new look at T cells. *J Exp Med* 187:1367–1371, 1998
17. Caruso A, Licenziati S, Corulli M, Canaris AD, De Francesco MA, Fiorentini S, Peroni L, Fallacara F, Dima F, Balsari A, Turano A: Flow cytometric analysis of activation markers on stimulated T cells and their correlation with cell proliferation. *Cytometry* 27:71–76, 1997
18. Kabelitz D, Oberg HH, Pohl T, Pechhold K: Antigen-induced death of mature T lymphocytes: analysis by flow cytometry. *Immunol Rev* 142:157–174, 1994
19. Dhein J, Walczak H, Baumler C, Debatin KM, Krammer PH: Autocrine T-cell suicide mediated by APO-1/(Fas/CD95). *Nature* 373:438–441, 1995
20. Boehme SA, Lenardo MJ: Propriocidal apoptosis of mature T lymphocytes occurs at S phase of the cell cycle. *Eur J Immunol* 23:1552–1560, 1993
21. Appel H, Seth NP, Gauthier L, Wucherpfennig KW: Anergy induction by dimeric TCR ligands. *J Immunol* 166:5279–5285, 2001
22. Harding CV, Unanue ER: Quantitation of antigen-presenting cell MHC class II/peptide complexes necessary for T-cell stimulation. *Nature* 346:574–576, 1990
23. Valitutti S, Muller S, Cella M, Padovan E, Lanzavecchia A: Serial triggering of many T-cell receptors by a few peptide-MHC complexes. *Nature* 375:148–151, 1995
24. Stefanova I, Dorfman JR, Germain RN: Self-recognition promotes the foreign antigen sensitivity of naive T lymphocytes. *Nature* 420:429–434, 2002
25. Wulfing C, Sumen C, Sjaastad MD, Wu LC, Dustin ML, Davis MM: Costimulation and endogenous MHC ligands contribute to T cell recognition. *Nat Immunol* 3:42–47, 2002
26. Irvine DJ, Purbhoo MA, Krogsgaard M, Davis MM: Direct observation of ligand recognition by T cells. *Nature* 419:845–849, 2002
27. Goldrath AW, Bevan MJ: Selecting and maintaining a diverse T-cell repertoire. *Nature* 402:255–262, 1999
28. Kotzin BL, Falta MT, Crawford F, Rosloniec EF, Bill J, Marrack P, Kappler J: Use of soluble peptide-DR4 tetramers to detect synovial T cells specific for cartilage antigens in patients with rheumatoid arthritis. *Proc Natl Acad Sci U S A* 97:291–296, 2000
29. Quarsten H, McAdam SN, Jensen T, Arentz-Hansen H, Molberg O, Lundin KE, Sollid LM: Staining of celiac disease-relevant T cells by peptide-DQ2 multimers. *J Immunol* 167:4861–4868, 2001
30. Liblau RS, Pearson CI, Shokat K, Tisch R, Yang XD, McDevitt HO: High-dose soluble antigen: peripheral T-cell proliferation or apoptosis. *Immunol Rev* 142:193–208, 1994
31. Renno T, Attinger A, Locatelli S, Bakker T, Vacheron S, MacDonald HR: Cutting edge: apoptosis of superantigen-activated T cells occurs preferentially after a discrete number of cell divisions in vivo. *J Immunol* 162:6312–6315, 1999
32. Ucker DS, Meyers J, Obermiller PS: Activation-driven T cell death. II. Quantitative differences alone distinguish stimuli triggering nontransformed T cell proliferation or death. *J Immunol* 149:1583–1592, 1992
33. Fahmy TM, Glick Bieler J, Edidin M, Schneck JP: Increased TCR avidity after T cell activation: a mechanism for sensing low-density antigen. *Immunity* 14:135–143, 2001
34. Herold KC, Hagopian W, Auger JA, Poumian-Ruiz E, Taylor L, Donaldson D, Gitelman SE, Harlan DM, Xu D, Zivin RA, Bluestone JA: Anti-CD3 monoclonal antibody in new-onset type 1 diabetes mellitus. *N Engl J Med* 346:1692–1698, 2002
35. Casares S, Hurtado A, McEvoy RC, Sarukhan A, von Boehmer H, Brumeanu TD: Down-regulation of diabetogenic CD4+ T cells by a soluble dimeric peptide-MHC class II chimera. *Nat Immunol* 3:383–391, 2002
36. Genain CP, Zamvil SS: Specific immunotherapy: one size does not fit all. *Nat Med* 6:1098–1100, 2000